CONTINGENCY DESIGNS FOR ATTITUDE DETERMINATION OF TRMM

John L. Crassidis, Stephen F. Andrews, F. Landis Markley
Goddard Space Flight Center, Code 712
Greenbelt, MD 20771

Kong Ha
Orbital Sciences Corporation
Greenbelt, MD 20770

Abstract

In this paper, several attitude estimation designs are developed for the Tropical Rainfall Measurement Mission (TRMM) spacecraft. A contingency attitude determination mode is required in the event of a primary sensor failure. The final design utilizes a full sixth-order Kalman filter. However, due to initial software concerns, the need to investigate simpler designs was required. The algorithms presented in this paper can be utilized in place of a full Kalman filter, and require less computational burden. These algorithms are based on filtered deterministic approaches and simplified Kalman filter approaches. Comparative performances of all designs are shown by simulating the TRMM spacecraft in mission mode. Comparisons of the simulation results indicate that comparable accuracy with respect to a full Kalman filter design is possible.

Introduction

The TRMM spacecraft is due to be launched in 1997 with a nominal mission lifetime of 42 months. The main objectives of this mission include: (1) to obtain multi-year measurements of tropical and subtropical rainfall, (2) to understand how interactions between the sea, air, and land masses produce changes in global rainfall and climate, and (3) to help improve the modeling of tropical rainfall processes and their influence on global circulation.

The spacecraft is three-axis stabilized in a near circular (350 km) orbit with an inclination of 35°. The nominal Earth-pointing mission mode requires a rotation once per orbit about the spacecraft's y-axis. The attitude determination hardware consists of an Earth Sensor Assembly (ESA), Digital Sun Sensors (DSS), Coarse Sun Sensors (CSS), a Three-Axis Magnetometer (TAM), and gyroscopic rate sensors. The attitude control hardware includes three Magnetic Torquer Bars (MTB) which are used to provide magnetic momentum unloading capability, and a Reaction Wheel Assembly (RWA) which consists of four wheels in a pyramidal arrangement to maximize momentum storage capability along a preferred axis.

Primary attitude determination is accomplished using the ESA and gyroscopes. The DSS is also used twice each orbit in order to update the yaw position estimate during mission pointing. The allotted attitude knowledge accuracy is 0.18° per axis. Simulation studies indicate that the primary attitude determination system meets the knowledge requirements [1]. In the event of an ESA failure, a contingency mode is used to allow for the continuation of the scientific mission. Attitude determination for the contingency mode is accomplished using the DSS, the TAM, and gyroscopes. The allotted attitude knowledge accuracy for the contingency mode is 0.7° per axis.

The algorithm chosen for the final contingency design incorporates a sixth-order Kalman filter [2]. This filter estimates both attitude error angles and gyro drift trajectories. However, due to initial concerns in software coding size and computations, the development of simpler and less software-intensive algorithms is required. A number of algorithms is presented in this paper, including: an

Isotropic Kalman Filter (IKF), a steady-state Angles-only Kalman Filter (AKF), an Enhanced TRIAD Algorithm (ETA), and an Enhanced QUEST Algorithm (EQA). All of these algorithms utilize magnetic field measurements, digital sun sensor measurements (when available), and gyro measurements. The IKF is a simplified Kalman filter in which an approximation is made where the rank deficient projection matrix is replaced by the identity matrix. This leads to attitude and gyro bias covariances that are the same in all directions in space. The AKF is a steady-state Kalman filter which estimates for angles only, with no gyro bias estimation. The ETA is essentially a first-order filter on TRIAD [3] determined attitudes. During solar eclipse, the ETA relies exclusively on model propagation using gyro measurements. Also, during sensor co-alignment the filter gain is automatically adjusted so that the filter relies more on the propagated attitude. The EQA is similar to the ETA, but uses the QUEST [4] algorithm for attitude determination. This allows for weighting of individual attitude sensor measurement sets.

The organization of this paper proceeds as follows. First, a summary of the spacecraft attitude kinematics is shown. Then, a brief review of the standard Kalman filter used for attitude estimation is shown. Next, the equations and properties of the IKF, AKF, ETA, and EQA are presented. Then, these algorithms are used to estimate the attitude of a simulated TRMM spacecraft. Finally, results are shown which compare each new algorithm to the full Kalman filter. A number of factors is considered, including: telemetry requirements, on-board requirements, coding size, and attitude accuracy.

Attitude Kinematics

In this section, a brief review of the kinematic and dynamic equations of motion for a three-axis stabilized spacecraft is shown. The attitude is assumed to be represented by the quaternion vector, defined as

$$\underline{q} \equiv \begin{bmatrix} \underline{q}_{13} \\ q_4 \end{bmatrix} \tag{1}$$

with

$$\underline{q}_{13} \equiv \begin{bmatrix} q_1 \\ q_2 \\ q_3 \end{bmatrix} = \underline{\hat{n}} \sin(\theta/2) \tag{2a}$$

$$q_4 = \cos(\theta/2) \tag{2b}$$

where $\underline{\hat{n}}$ is a unit vector corresponding to the axis of rotation and θ is the angle of rotation. The quaternion kinematic equations of motion are derived by using the spacecraft's angular velocity ($\underline{\omega}$), given by

$$\dot{\underline{q}} = \frac{1}{2}\Omega(\underline{\omega})\underline{q} = \frac{1}{2}\Xi(\underline{q})\underline{\omega} \tag{3}$$

where $\Omega(\underline{\omega})$ and $\Xi(\underline{q})$ are defined as

$$\Omega(\underline{\omega}) \equiv \begin{bmatrix} -[\underline{\omega}\times] & \vdots & \underline{\omega} \\ \cdots\cdots & \vdots & \cdots\cdots \\ -\underline{\omega}^T & \vdots & 0 \end{bmatrix} \tag{4a}$$

$$\Xi(\underline{q}) \equiv \begin{bmatrix} q_4 I_{3\times 3} + [\underline{q}_{13}\times] \\ \cdots\cdots\cdots\cdots \\ -\underline{q}_{13}^T \end{bmatrix} \tag{4b}$$

The 3×3 dimensional matrices $\left[\underline{\omega}\times\right]$ and $\left[\underline{q}_{13}\times\right]$ are referred to as cross product matrices since $\underline{a}\times\underline{b}=\left[\underline{a}\times\right]\underline{b}$, with

$$\left[\underline{a}\times\right]\equiv\begin{bmatrix}0 & -a_3 & a_2\\ a_3 & 0 & -a_1\\ -a_2 & a_1 & 0\end{bmatrix} \tag{5}$$

Since a three degree-of-freedom attitude system is represented by a four-dimensional vector, the quaternions cannot be independent. This condition leads to the following normalization constraint

$$\underline{q}^T\underline{q}=\underline{q}_{13}^T\underline{q}_{13}+q_4^2=1 \tag{6}$$

The measurement model is assumed to be of the form given by

$$\underline{B}_B=A\left(\underline{q}\right)\underline{B}_I \tag{7}$$

where $\underline{B}_I$ is a 3×1 dimensional vector of some reference object (e.g., a vector to the sun or to a star, or the Earth's magnetic field vector) in a reference coordinate system, $\underline{B}_B$ is a 3×1 dimensional vector defining the components of the corresponding reference vector measured in the spacecraft body frame, and $A\left(\underline{q}\right)$ is given by

$$A\left(\underline{q}\right)=\left(q_4^2-\underline{q}_{13}^T\underline{q}_{13}\right)I_{3\times 3}+2\,\underline{q}_{13}\underline{q}_{13}^T-2\,q_4\left[\underline{q}_{13}\times\right] \tag{8}$$

which is the 3×3 dimensional (orthogonal) attitude matrix.

Kalman Filter Review

In this section, a review of the basic principles of the Kalman filter applied to attitude estimation is shown (see [2] for more details). The state error vector has seven components consisting of a four-component error quaternion ($\delta\underline{q}$) and a three-vector gyro bias error $\Delta\underline{b}$, given by

$$\Delta\underline{x}=\begin{bmatrix}\delta\underline{q}\\ ---\\ \Delta\underline{b}\end{bmatrix} \tag{9}$$

The error quaternion is defined as

$$\delta\underline{q}=\underline{q}\otimes\hat{\underline{q}}^{-1} \tag{10}$$

where $\underline{q}$ is the true quaternion and $\hat{\underline{q}}$ is the estimated quaternion. Also, the operator $\otimes$ refers to quaternion multiplication (see [3] for details). Since the incremental quaternion corresponds to a small rotation, Equation (10) can be approximated by

$$\delta\underline{q}\approx\begin{bmatrix}\delta\underline{q}_{13}\\ 1\end{bmatrix} \tag{11}$$

which reduces the four-component error quaternion into a three-component (half-angle) representation.

The true angular velocity is assumed to be modeled by

$$\underline{\omega} = \underline{\omega}_g - \underline{b} - \underline{\eta}_1 \tag{12}$$

where $\underline{\omega}$ is the true angular velocity, $\underline{\omega}_g$ is the gyro-determined angular velocity, and $\underline{b}$ is the gyro drift vector, which is modeled by

$$\dot{\underline{b}} = \underline{\eta}_2 \tag{13}$$

The 3×1 vectors, $\underline{\eta}_1$ and $\underline{\eta}_2$, are assumed to be modeled by a Gaussian white-noise process with

$$E\left\{\underline{\eta}_i(t)\right\} = \underline{0} \qquad i = 1, 2 \tag{14a}$$

$$E\left\{\underline{\eta}_i(t)\underline{\eta}_j^T(t')\right\} = Q_i\, \delta_{ij}\, \delta(t - t') \qquad i, j = 1, 2 \tag{14b}$$

Using the reduced error quaternion in Equation (11) and the gyro drift model in Equation (13), the state error equation may be written as [2]

$$\Delta\dot{\underline{x}} = F\, \Delta\underline{x} + G\, \underline{w} \tag{15}$$

where

$$F = \begin{bmatrix} -[\hat{\underline{\omega}}\times] & -\frac{1}{2} I_{3\times 3} \\ 0_{3\times 3} & 0_{3\times 3} \end{bmatrix} \tag{16a}$$

$$G = \begin{bmatrix} -\frac{1}{2} I_{3\times 3} & 0_{3\times 3} \\ 0_{3\times 3} & I_{3\times 3} \end{bmatrix} \tag{16b}$$

$$\underline{w} = \begin{bmatrix} \underline{\eta}_1 \\ \underline{\eta}_2 \end{bmatrix} \tag{16c}$$

$$\hat{\underline{\omega}} = \underline{\omega}_g - \hat{\underline{b}} \tag{16d}$$

State-observable discrete measurements are assumed to be modeled by

$$\underline{z}_k = h_k(\underline{x}_k) + \underline{\nu}_k \tag{17}$$

where

$$h_k(\underline{x}_k) = A(\underline{q}_k)\, \underline{B}_{I_k} \tag{18}$$

and $\underline{\nu}_k$ is assumed to be modeled by a zero-mean Gaussian process with

$$E\left\{\underline{\nu}_k\right\} = \underline{0} \tag{19a}$$

$$E\left\{\underline{\nu}_k\, \underline{\nu}_l^T\right\} = \delta_{kl}\, R_k \tag{19b}$$

The sensitivity matrix can be written as

$$H_k = \left[\underline{l}_k \quad \vdots \quad 0_{3\times 3} \right] \tag{20}$$

where

$$\underline{l}_k = 2\left[A\left(\hat{\underline{q}}\right) \underline{B}_I \times \right]_k \tag{21}$$

The extended Kalman filter equations for attitude estimation are summarized by

$$\dot{P} = F\,P + P^T F + G\,Q\,G^T \tag{22a}$$

$$\Delta\hat{\underline{x}}_k = K_k \left[\underline{z}_k - h_k\left(\hat{\underline{q}}_k(-)\right) \right] \tag{22b}$$

$$P_k(+) = \left[I_{6\times 6} - K_k\, H_k\left(\hat{\underline{x}}_k(-)\right) \right] P_k(-) \tag{22c}$$

$$K_k = P_k(-)\, H_k^T \left[H_k\, P_k(-)\, H_k^T + R_k \right]^{-1} \tag{22d}$$

$$\hat{\underline{q}}(+) = \delta\hat{\underline{q}}(+) \otimes \hat{\underline{q}}(-) \tag{22e}$$

$$\hat{\underline{b}}(+) = \hat{\underline{b}}(-) + \Delta\hat{\underline{b}}(+) \tag{22f}$$

$$\delta\hat{\underline{q}}(+) = \begin{bmatrix} \delta\hat{\underline{q}}_{13}(+) \\ 1 \end{bmatrix} \tag{22g}$$

Isotropic Kalman Filter

In this section, the equations for the IKF are shown. The state vector consists of an incremental quaternion and gyro bias. The gyro propagation portion of the IKF is identical to the full Kalman filter shown in the previous section. However, the assumed measurement in the IKF is given by

$$\tilde{\underline{z}} = \tilde{\underline{u}} \times \hat{\underline{u}} \tag{23}$$

where $\tilde{\underline{u}}$ is the measured unit vector from either the TAM or DSS in the body frame, and $\hat{\underline{u}}$ is the corresponding expected value, obtained by mapping the inertial reference to the body-fixed coordinate system using the estimated quaternion. Also, from Equation (23) $\hat{\underline{z}} = \underline{0}$, since the cross product of a vector with itself is zero. The sensitivity matrix of the measurement model in Equation (23) is determined by using the attitude matrix of the angle error. This leads to

$$\tilde{\underline{u}} = A\left(\underline{\alpha}\right) \hat{\underline{u}} \tag{24}$$

where $\underline{\alpha}$ is an incremental error angle. Using the approximation

$$A\left(\underline{\alpha}\right) = I_{3\times 3} - \left[\underline{\alpha} \times\right] \tag{25}$$

leads to the following measurement model

$$\tilde{\underline{z}} = \left(I_{3\times 3} - \hat{\underline{u}}\,\hat{\underline{u}}^T \right) \underline{\alpha} \tag{26}$$

Therefore, the sensitivity matrix, which contains partials with respect to the error state, is given by

$$H = \begin{bmatrix} H_u & \vdots & 0_{3\times 3} \end{bmatrix} \tag{27}$$

where

$$H_u = I_{3\times 3} - \underline{\hat{u}}\,\underline{\hat{u}}^T \tag{28}$$

This matrix is the projection operator onto the space perpendicular to $\underline{\hat{u}}$, which reflects the fact that an observation of a unit vector contains no information about rotations around an axis specified by that vector. Therefore, H_u has rank two. Also, if the measurement errors for each sensor are assumed equal in all directions, then the measurement error covariance is given by

$$R = r\, H_u \tag{29}$$

where r is a scalar. Equation (29) indicates that there is no uncertainty in the length of the measured vector. The IKF is derived by making an approximation of replacing the rank-two sensitivity matrix in Equation (28) by the rank-three identity matrix, which leads to

$$H_u = I_{3\times 3} \tag{30a}$$

$$R = r\, I_{3\times 3} \tag{30b}$$

This approximation leads to attitude and gyro bias covariances which are equal in all directions in space, or *isotropic*. Therefore, the covariance matrix has the form given by

$$P = \begin{bmatrix} p_a\, I_{3\times 3} & p_c\, I_{3\times 3} \\ p_c\, I_{3\times 3} & p_b\, I_{3\times 3} \end{bmatrix} \tag{31}$$

where P_a, P_c, and P_b are scalar quantities. Also, the state transition matrix is approximated by

$$\Phi = \begin{bmatrix} I_{3\times 3} & -\Delta t\, I_{3\times 3} \\ 0_{3\times 3} & I_{3\times 3} \end{bmatrix} \tag{32}$$

where Δt is the sampling interval. Equation (32) ignores spacecraft rotation, which is irrelevant since the covariance matrix in Equation (31) is isotropic. The covariance propagation equations are now given by

$$p_{a_{k+1}}(-) = p_{a_k}(+) - 2p_{c_k}(+)\Delta t + p_{b_k}(+)\Delta t^2 + \sigma_v^2 \Delta t + \frac{1}{3}\sigma_u^2 \Delta t^3 \tag{33a}$$

$$p_{c_{k+1}}(-) = p_{c_k}(+) - p_{b_k}(+)\Delta t - \frac{1}{2}\sigma_u^2 \Delta t^2 \tag{33b}$$

$$p_{b_{k+1}}(-) = p_{b_k}(+) + \sigma_u^2 \Delta t \tag{33c}$$

where σ_u^2 and σ_v^2 are the scalar covariances of the gyro-drift ramp noise, and the gyro-drift rate measurement noise, respectively. The Kalman gain matrix is given by

$$K = \begin{bmatrix} k_a\, I_{3\times 3} & \vdots & k_b\, I_{3\times 3} \end{bmatrix}^T \tag{34}$$

where

$$k_a = \frac{p_{a_{k+1}}(-)}{p_{a_{k+1}}(-) + r} \tag{35a}$$

$$k_b = \frac{p_{c_{k+1}}(-)}{p_{a_{k+1}}(-) + r} \tag{35b}$$

Therefore, the Kalman covariance and state update equations are given by

$$p_{a_{k+1}}(+) = r\, k_a \tag{36a}$$

$$p_{c_{k+1}}(+) = r\, k_b \tag{36b}$$

$$p_{b_{k+1}}(+) = p_{b_{k+1}}(-) - k_b p_{c_{k+1}}(-) \tag{36c}$$

$$\underline{\hat{q}}_{k+1}(+) = \begin{bmatrix} \frac{1}{2} k_a (\underline{\tilde{u}} \times \underline{\hat{u}}) \\ 1 \end{bmatrix} \otimes \underline{\hat{q}}_{k+1}(-) \tag{37a}$$

$$\underline{\hat{b}}_{k+1}(+) = \underline{\hat{b}}_{k+1}(-) + k_b (\underline{\tilde{u}} \times \underline{\hat{u}}) \tag{37b}$$

Since, Equations (37a) and (37b) depend on the cross product measurement $(\underline{\tilde{u}} \times \underline{\hat{u}})$, the updates to the quaternions and biases are still perpendicular to $\underline{\hat{u}}$ despite the approximation to the sensitivity matrix.

Steady-State Angles-only Kalman Filter

In this section, a simplified version of the full Kalman filter is shown. The AKF estimates only the quaternion, and not the gyro drift. The covariance and state transition matrices are the upper 3×3 blocks of the corresponding matrices in a full Kalman filter. Therefore, covariance propagation is given by

$$P_{k+1}(-) = \Phi\, P_k(+) \Phi + w\, I_{3\times 3} \tag{38}$$

where w is the assumed scalar level of the process noise. A full angles-only Kalman filter rapidly approaches steady-state using the covariance propagation in Equation (38). Therefore, a steady-state covariance is used. An investigation of the eigenvalues of the covariance matrix shows that there is one large eigenvalue (p_{max}), and two nearly equal smaller eigenvalues (p_{min}). Also, the eigenvector corresponding to p_{max} is found to always be within 2.5 degrees of the sun vector in the body. This reflects the fact that the more accurate sun sensor cannot reduce attitude errors along the sun line, which must be estimated using the less-accurate TAM. Therefore, the covariance matrix is given by

$$P = p_{eye}\, I_{3\times 3} + p_{sun}\, \underline{s}\, \underline{s}^T \tag{39}$$

where $\underline{s}$ is the sun vector in the body frame, and p_{eye} and p_{sun} are constants. The minimum eigenvalue is given by p_{eye}, and the maximum eigenvalue is given by $p_{eye} + p_{sun}$.

Sun Sensor Update

The sensitivity matrix and measurement covariance for the sun sensor are given by

$$H_s = [\underline{\hat{s}} \times] \tag{40a}$$

$$R_s = r_s\, I_{3\times 3} \tag{40b}$$

where $\underline{\hat{s}}$ is the estimated sun vector in the body frame, and r_s is the scalar (isotropic) measurement covariance. The Kalman gain for the sun sensor update requires the computation of

$$\left\{H_s P H_s^T + R_s\right\}^{-1} = \left\{p_{eye}\left[\underline{\hat{s}}\times\right]\left[\underline{\hat{s}}\times\right]^T + p_{sun}\left(\underline{\hat{s}}\times\underline{\hat{s}}\right)\left(\underline{\hat{s}}\times\underline{\hat{s}}\right)^T + R_s\right\}^{-1}$$
$$= \frac{1}{r_s + p_{eye}}\left\{I_{3\times 3} + \frac{p_{eye}\,\underline{\hat{s}}\,\underline{\hat{s}}^T}{r_s}\right\} \tag{41}$$

Therefore, the Kalman gain matrix is given by

$$K_s = P H_s^T\left\{H_s P H_s^T + R_s\right\}^{-1}$$
$$= \frac{1}{r_s + p_{eye}}\left\{p_{eye}\, I_{3\times 3} + p_{sun}\,\underline{\hat{s}}\,\underline{\hat{s}}^T\right\}\left[\underline{\hat{s}}\times\right]^T\left\{I_{3\times 3} + \frac{p_{eye}\,\underline{\hat{s}}\,\underline{\hat{s}}^T}{r_s}\right\} \tag{42}$$
$$= \frac{p_{eye}}{r_s + p_{eye}}\left[\underline{\hat{s}}\times\right]^T$$

If the measurements are processed at a given time by accumulating an incremental error angle $\underline{\alpha}$ initialized at zero, without re-computing the quaternion between updates, the state update becomes

$$\underline{\alpha}(+) = \underline{\alpha}(-) + \frac{p_{eye}}{r_s + p_{eye}}\left\{\underline{\tilde{s}}\times\underline{\hat{s}} - \left(I_{3\times 3} - \underline{\hat{s}}\,\underline{\hat{s}}^T\right)\underline{\alpha}(-)\right\} \tag{43}$$

where $\underline{\tilde{s}}$ is the measured sun vector in the body frame.

TAM Update

The sensitivity matrix and measurement covariance for the TAM are given by

$$H_t = \left[\underline{\hat{m}}\times\right] \tag{44a}$$
$$R_t = r_t\, I_{3\times 3} \tag{44b}$$

where $\underline{\hat{m}}$ is the estimated magnetic field vector in the body frame, and r_t is the scalar (isotropic) measurement covariance. The Kalman gain for the TAM update requires the computation of

$$\left\{H_t P H_t^T + R_t\right\}^{-1} = \left\{p_{eye}\left[\underline{\hat{m}}\times\right]\left[\underline{\hat{m}}\times\right]^T + p_{sun}\left(\underline{\hat{m}}\times\underline{\hat{s}}\right)\left(\underline{\hat{m}}\times\underline{\hat{s}}\right)^T + R_t\right\}^{-1} \tag{45}$$

The inverse in Equation (45) is computable in closed form, but is complicated. An approximation is made which assumes r_t is much larger than both p_{eye} and p_{sun}. Therefore, Equation (45) is re-written as

$$\left\{H_t P H_t^T + R_t\right\}^{-1} \approx \frac{1}{r_t} I_{3\times 3} \tag{46}$$

The Kalman gain matrix is now given by

$$K_t = P H_t^T\left\{H_t P H_t^T + R_t\right\}^{-1}$$
$$\approx \frac{1}{r_t}\left\{p_{eye}\, I_{3\times 3} + p_{sun}\,\underline{\hat{s}}\,\underline{\hat{s}}^T\right\}\left[\underline{\hat{m}}\times\right]^T \tag{47}$$

The state update is given by

$$\underline{\alpha}(+) = \underline{\alpha}(-) + \frac{1}{r_t}\left\{p_{eye}\, I_{3\times 3} + p_{sun}\, \hat{\underline{s}}\, \hat{\underline{s}}^T\right\}\left\{\tilde{\underline{m}} \times \hat{\underline{m}} - \left(\hat{\underline{m}}^T\, \hat{\underline{m}}\, I_{3\times 3} - \hat{\underline{m}}\, \hat{\underline{m}}^T\right)\underline{\alpha}(-)\right\} \tag{48}$$

where $\tilde{\underline{m}}$ is the measured TAM vector in the body frame.

Enhanced TRIAD and QUEST Algorithms

In this section, the ETA and EQA are developed. These algorithms are essentially based on an "alpha-type" [5] filter applied to deterministic methods. The TRIAD algorithm [3] involves the construction of two triads from a pair of orthonormal vectors, $\underline{u}$ and $\underline{v}$, with basis vectors given by

$$\underline{l} = \underline{u} \tag{49a}$$

$$\underline{m} = \frac{\underline{u} \times \underline{v}}{|\underline{u} \times \underline{v}|} \tag{49b}$$

$$\underline{n} = \underline{l} \times \underline{m} \tag{49c}$$

The basis vectors are constructed for both body measured vectors $\underline{u}_B$ and $\underline{v}_B$, and for the inertial reference vectors $\underline{u}_I$ and $\underline{v}_I$. Two orthogonal 3×3 matrices are then constructed, given by

$$M_B = \left[\underline{l}_B \quad \underline{m}_B \quad \underline{n}_B\right] \tag{50a}$$

$$M_I = \left[\underline{l}_I \quad \underline{m}_I \quad \underline{n}_I\right] \tag{50b}$$

The attitude matrix maps the inertial reference to the body frame, and can be determined by

$$A = M_B M_I^T \tag{51}$$

An accurate method for extracting the quaternions from the attitude matrix is given in [6].

The TRIAD method (as well as all deterministic) methods requires at least two sets of vector measurements to determine the attitude matrix. This method subsequently fails when only one set of vector measurements (e.g., TAM data only) is available. Also, deterministic methods fail when vectors are co-aligned (i.e., $|\underline{u} \cdot \underline{v}| = 1$). These difficulties are overcome by combining the TRIAD determined quaternions with a gyro-propagated model and a simple first-order filter. The ETA is given by

$$\underline{q}_p(+) = \exp\left\{\frac{1}{2}\Omega\left(\tilde{\underline{\omega}}_g\right)\Delta t\right\}\hat{\underline{q}}(-) \tag{52a}$$

$$\hat{\underline{q}}(+) = (1-\alpha)\,\underline{q}_p(+) + \alpha\, \underline{q}_{triad}(+) \tag{52b}$$

where $\underline{q}_p$ is the propagated quaternion, $\hat{\underline{q}}$ is the estimated quaternion, and $\underline{q}_{triad}$ is the quaternion extracted from the TRIAD determined attitude matrix. The scalar gain variable α is given by

$$\alpha = |\underline{u} \times \underline{v}|^2\, \alpha_0 \tag{53}$$

where α_0 is a constant gain. The filter gain in Equation (53) is automatically adjusted to accommodate periods of vector co-alignment (i.e., as the vectors become co-aligned, the gain approaches 0). Also, α_0 is set to zero when only one measurement set is available.

The ETA is essentially a first-order "additive" Kalman filter. In general, this approach will not maintain quaternion normalization [7]. To investigate how the ETA affects quaternion normalization, Equation (52b) may be re-written as

$$\hat{\underline{q}} = \underline{q}_p \otimes \left[I_q + \alpha \left(\underline{q}_p^{-1} \otimes \underline{q}_{triad} - I_q \right) \right] \tag{54}$$

where I_q is the identity quaternion. If the propagated quaternion is close to the TRIAD determined quaternion, then Equation (54) can be approximated accurately by

$$\hat{\underline{q}} \approx \underline{q}_p \otimes \begin{bmatrix} \frac{1}{2} \alpha \, \delta\underline{\theta} \\ 1 \end{bmatrix} \tag{55}$$

where $\delta\underline{\theta}$ is the angle vector between $\underline{q}_p$ and $\underline{q}_{triad}$. Therefore, since α_0 is very small, normalization is maintained to within first-order. For numerical precision, the quaternions are explicitly normalized.

The EQA is similar to the ETA, but uses the QUEST [4] algorithm to determine attitude. The QUEST algorithm minimizes the following cost function [8]

$$L(A) = \frac{1}{2} \sum_{k=1}^{n} a_k \left| \underline{w}_k - A \underline{v}_k \right|^2 \tag{56}$$

where $\underline{w}$ is a set of unit vector observations in the body-frame, $\underline{v}$ is a set of unit observations with respect to the inertial frame, and n is the total number of vector measurement sets. The constants a_k serve to weight individual sensor measurements. Shuster [4] has shown that the maximum-likelihood estimate of the attitude is obtained with weights given by

$$a_k = \frac{1}{\sigma_k^2} \tag{57}$$

where σ_k is the standard-deviation of the measurement error process for each sensor.

TRMM Simulation and Results

In order to compare the algorithms developed in this paper, a simulation study is performed using TRMM orbit parameters and performance criteria. The simulated spacecraft has a near circular orbit at 350 km, and completes an orbit in approximately 90 minutes. The nominal mission mode requires a rotation once per orbit (i.e., 236 deg/hr) about the spacecraft's y-axis while holding the remaining axis rotations near zero. The "true" magnetic field reference is modeled using a 10th order International Geomagnetic Reference Field (IGRF) model. In order to simulate magnetic field modeling error, a 6th order IGRF is used to develop "measurements." TAM sensor noise is modeled by a Gaussian white-noise process with a mean of zero and a standard deviation of 0.5 mG. The two DSS's each have a field of view of about 50° × 50°. The body to sensor transformations for each sensor is given by

$$T_1 = \begin{bmatrix} -0.5736 & 0 & -0.8192 \\ 0.4096 & 0.866 & -0.2868 \\ 0.7094 & -0.5 & -0.4967 \end{bmatrix} \tag{58a}$$

$$T_2 = \begin{bmatrix} -0.5736 & 0 & 0.8192 \\ -0.4096 & 0.866 & -0.2868 \\ -0.7094 & -0.5 & -0.4967 \end{bmatrix} \tag{58b}$$

Each DSS views the sun when the sensor view is greater than the cosine of 50°. The two DSS's combine to provide sun measurements for about 2/3 of a complete orbit. The DSS sensor noise is also modeled by a Gaussian white-noise process with a mean of zero and a standard deviation of 0.05°. The gyro "measurements" are simulated using Equations (12) and (13), with a gyro noise standard deviation

of 0.062 deg/hr, a ramp noise standard deviation of 0.235 deg/hr/hr, and an initial drift of -0.1 deg/hr on each axis.

A plot of the roll, pitch, and yaw attitude errors for a typical simulation run using the full Kalman filter is shown in Figure 1. A plot of the corresponding gyro-bias estimates is shown in Figure 2. From Figure 1, the roll and yaw attitude errors show a strong dependence on orbit rate which is centered at zero, and a pitch error which is biased. This error bias may be due to non-Gaussian modeling errors in the magnetic field "measurements." These nonlinearities cause an error in inertial space which is not zero-mean and is largely along the sun line. When these errors are mapped into the body frame, sinusoidal motions occur in roll and yaw which are 90° out of phase from each other. Also, a biased error occurs in pitch which has the same magnitude as the sinusoidal motion, since the sun vector is 45° off the pitch axis. This can be shown mathematically by redefining an inertial reference fixed on the orbit plane with the x-axis tangent to the orbit plane, the z-axis pointed nadir, and the y-axis completing the triad. For a zero rotation, the inertial reference corresponds to the body frame. Therefore, from Figure 1 a starting value for the inertial reference can be chosen such that the z-axis is zero, and the remaining axes equal in magnitude. The mapping to the body frame for a rotation about the y-axis is given by

$$\underline{e} = \delta \begin{bmatrix} \cos(\mu) & 0 & \sin(\mu) \\ 0 & 1 & 0 \\ -\sin(\mu) & 0 & \cos(\mu) \end{bmatrix} \underline{s} = \frac{1}{\sqrt{2}} \begin{bmatrix} \cos(\mu) \\ 1 \\ -\sin(\mu) \end{bmatrix} \tag{59}$$

where μ is the true anomaly, δ is the magnitude of the error, and $\underline{s}$ is the direction of the sun vector, given by.

$$\underline{s} = \begin{bmatrix} 1 \\ 1 \\ 0 \end{bmatrix} \tag{60}$$

Clearly, a sinusoidal motion and constant bias is shown by Equation (59). This effect is also seen when using a Kalman filter on other spacecraft (e.g., UARS and SAMPEX). However, the full Kalman filter is able to estimate attitudes to within 0.1°, and estimates the gyro-drift fairly accurately.

A plot of the attitude errors for a typical simulation run using the IKF is shown in Figure 3. There is no clear orbit rate dependence in roll and yaw for this algorithm, but all angle errors are now biased. This may be due to the fact that the IKF assumes that the attitude covariance is equal in all directions, so that any biased errors are translated into all axes. The gyro-bias estimates (shown in Figure 4) are estimated more accurately using the IKF, as compared to the full Kalman filter. However, comparing magnitude attitude errors in Figure 3 to Figure 1 shows that attitude accuracy is no better than the full Kalman filter.

A plot of the attitude errors using the AKF is shown in Figure 5. The errors in roll and pitch are biased, while the yaw error has a mean near zero. These errors are likely due to not correcting for gyro bias in the filter. This is further depicted in the attitude covariance matrix, which is an order of magnitude larger than the full Kalman filter attitude covariance. However, attitude accuracy is still comparable to the full Kalman filter (i.e., within 0.1°).

A plot of the attitude errors using the ETA is shown in Figure 6. The peak errors seen predominately in the pitch and yaw errors are due to periods of sun un-observability. During these periods, the filter gain (shown in Figure 7) is set to zero, so that attitude is determined from gyro-propagation solely. Also, the gain clearly shows a sinusoidal motion. This motion compensates for measurement vector co-alignment. Attitude accuracy for this simple approach is within 0.15°. Also, the EQA improves the attitude accuracy slightly, but not to any appreciable amount.

Table 1 shows a summary of telemetry requirements, on-board table (initialization) requirements, code size, and performance results for each algorithm described in this paper. Clearly, comparable

performance with respect to the full Kalman filter is possible using either the IKF or AKF. Also, the AKF requires less telemetry and table values, and requires less coding size than either the full Kalman filter or the IKF. The ETA requires the least amount of telemetry and table values, and requires the least amount of coding. Even though attitude accuracy is slightly degraded as compared to the full Kalman filter, the simulation study indicates that the 0.7° attitude knowledge requirement is clearly met.

Table 1 Telemetry and Table Values, Code Size, and Performance

	Full KF	IKF	AKF	EQA	ETA
Telemetry	~40 values	~25 values	~15 values	~5 values	~5 values
Table	~30 values	~20 values	~15 values	~8 values	~5 values
Code Size	<6 K	<4K	<4 K	<2 K	<1 K
Performanc	<0.1°	<0.1°	<0.1°	<0.14°	<0.15°

Conclusions

A number of alternatives to using a full Kalman filter for attitude estimation was presented in this paper. In order to quantify the performance of these proposed algorithms, a simulation study was performed for the TRMM spacecraft. The results of this simulation study indicated that comparable accuracy with respect to a full Kalman filter design is possible. In particular, the ETA was shown to be an effective attitude estimator, while at the same time dramatically decreasing coding size, and telemetry and on-board requirements. Although the full Kalman filter was chosen for the final contingency mode of TRMM, the study presented in this paper provided valuable alternatives for future attitude estimation schemes.

Acknowledgment

The first author's work was supported by a National Research Council Postdoctoral Fellowship tenured at NASA-Goddard Space Flight Center. The author greatly appreciates this support.

References

[1] *TRMM Attitude Control Subsystem Specifications*, NASA-Goddard Space Flight Center (GSFC-TRMM-712-046).

[2] Lefferts, E.J., Markley, F.L., and Shuster, M.D., "Kalman Filtering for Spacecraft Attitude Estimation," *Journal of Guidance, Control and Dynamics*, Vol. 5, No. 5, Sept.-Oct. 1982, pp. 417-429.

[3] Wertz, J.S. (ed.), *Spacecraft Attitude Determination and Control*, D. Reidel Publishing Co., Dordrecht, The Netherlands, 1984.

[4] Shuster, M.D., and Oh, S.D., "Three-Axis Attitude Determination from Vector Observations," *Journal of Guidance and Control*, Vol. 4, No. 1, Jan.-Feb. 1981, pp. 70-77.

[5] Crassidis, J.L., Mook, D.J., and McGrath, J.M., "Automatic Carrier Landing System Utilizing Aircraft Sensors," *Journal of Guidance, Dynamics and Control*, Vol. 16, No. 5, Sept.-Oct. 1993, pp. 914-921.

[6] Sheppard, S.W., "Quaternion from Rotation Matrix," *Journal of Guidance and Control*, Vol. 1, No. 3, May-June 1978, pp. 223-224.

[7] Bar-Itzhack, I.Y., and Deutschmann, J.K., "Extended Kalman Filter for Attitude Estimation of the Earth Radiation Budget Satellite," *Proceedings of the AAS Astrodynamics Conference*, Portland, OR, August 1990, AAS Paper #90-2964, pp. 786-796.

[8] Wahba, G., "A Least-Squares Estimate of Satellite Attitude," Problem 65-1, *SIAM Review*, Vol. 7, No. 3, July 1965, pg. 409.

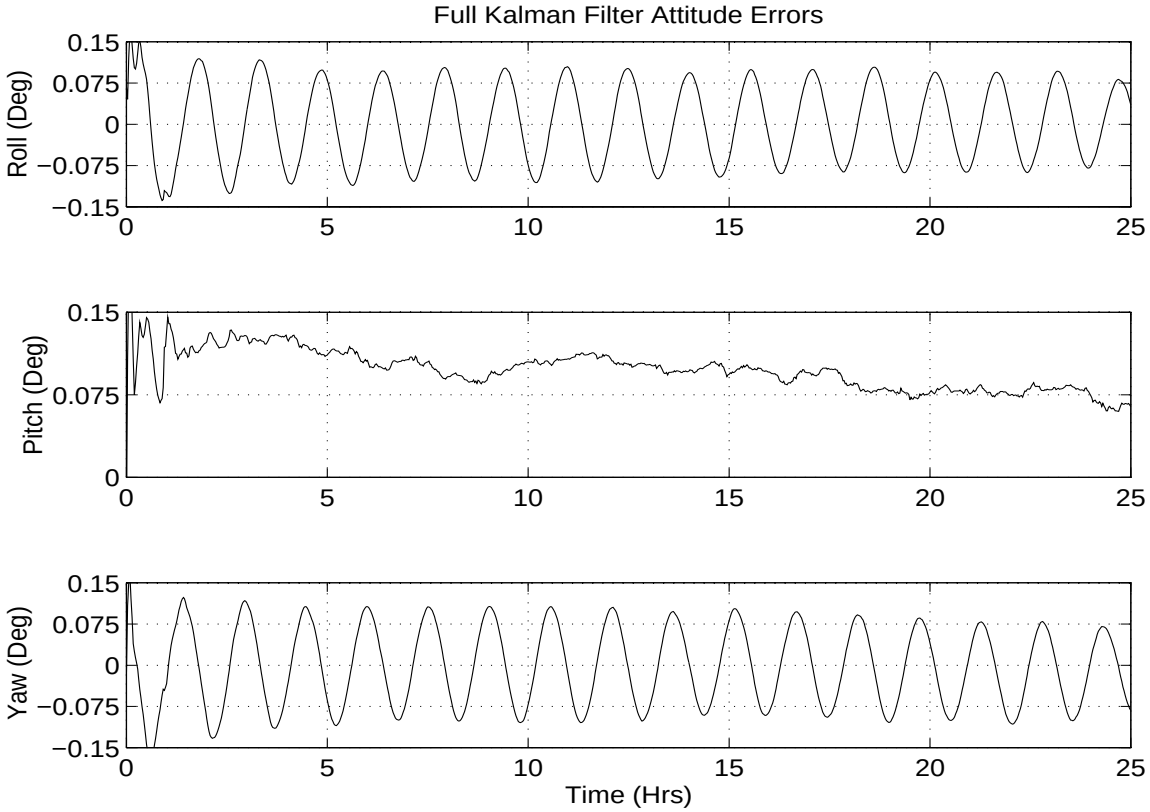

Figure 1 Kalman Filter Attitude Errors

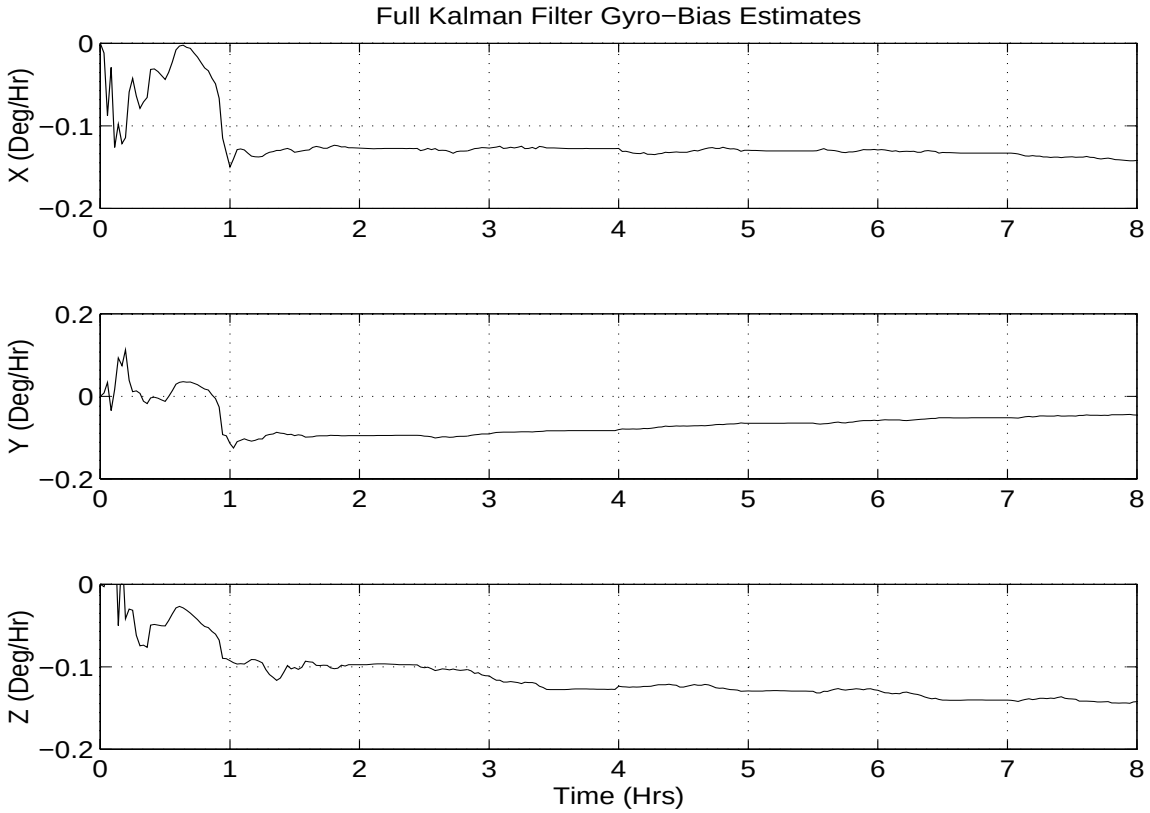

Figure 2 Kalman Filter Gyro Bias Estimates

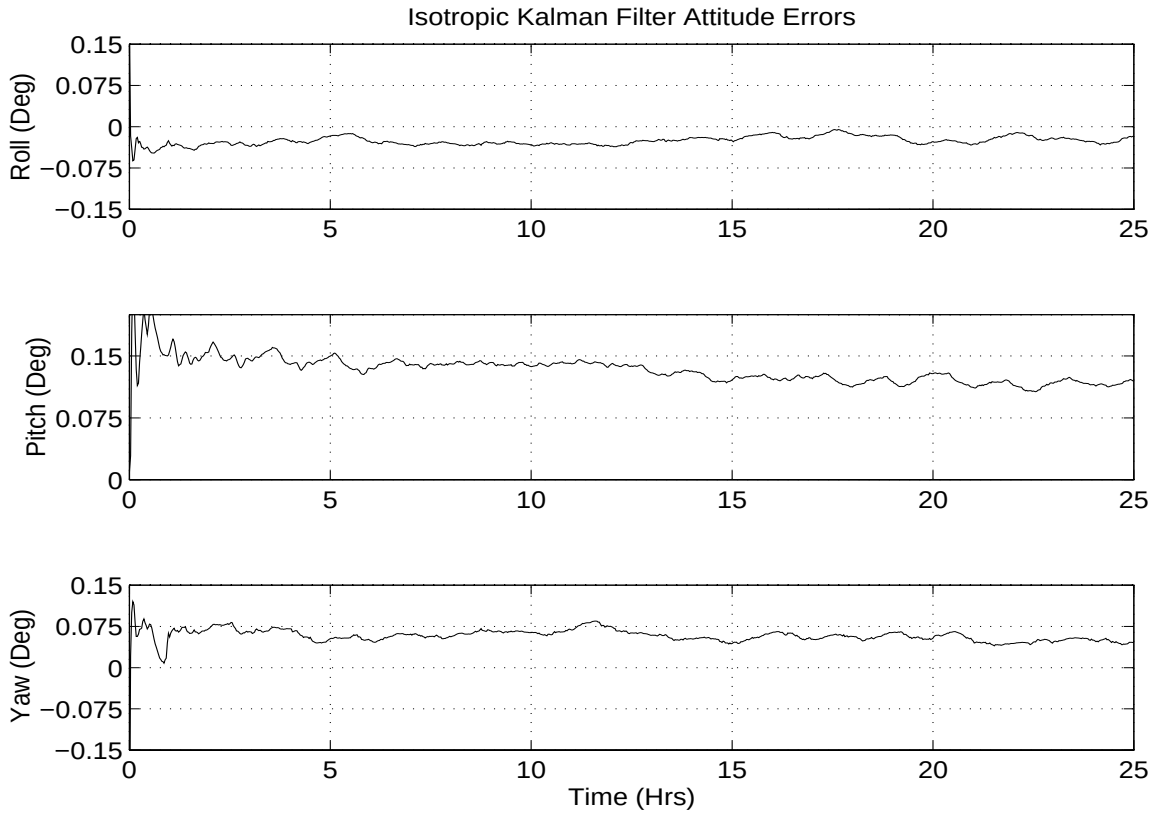

Figure 3 Isotropic Kalman Filter Attitude Errors

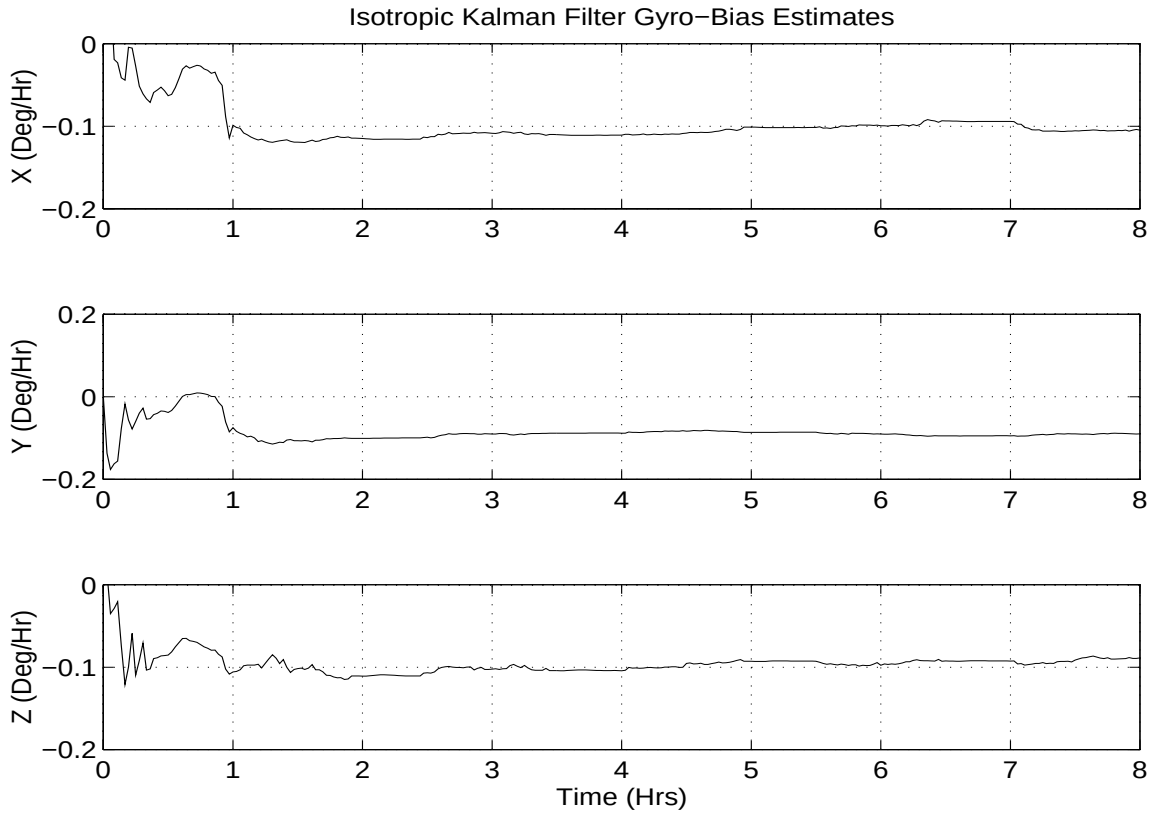

Figure 4 Isotropic Kalman Filter Gyro Bias Estimates

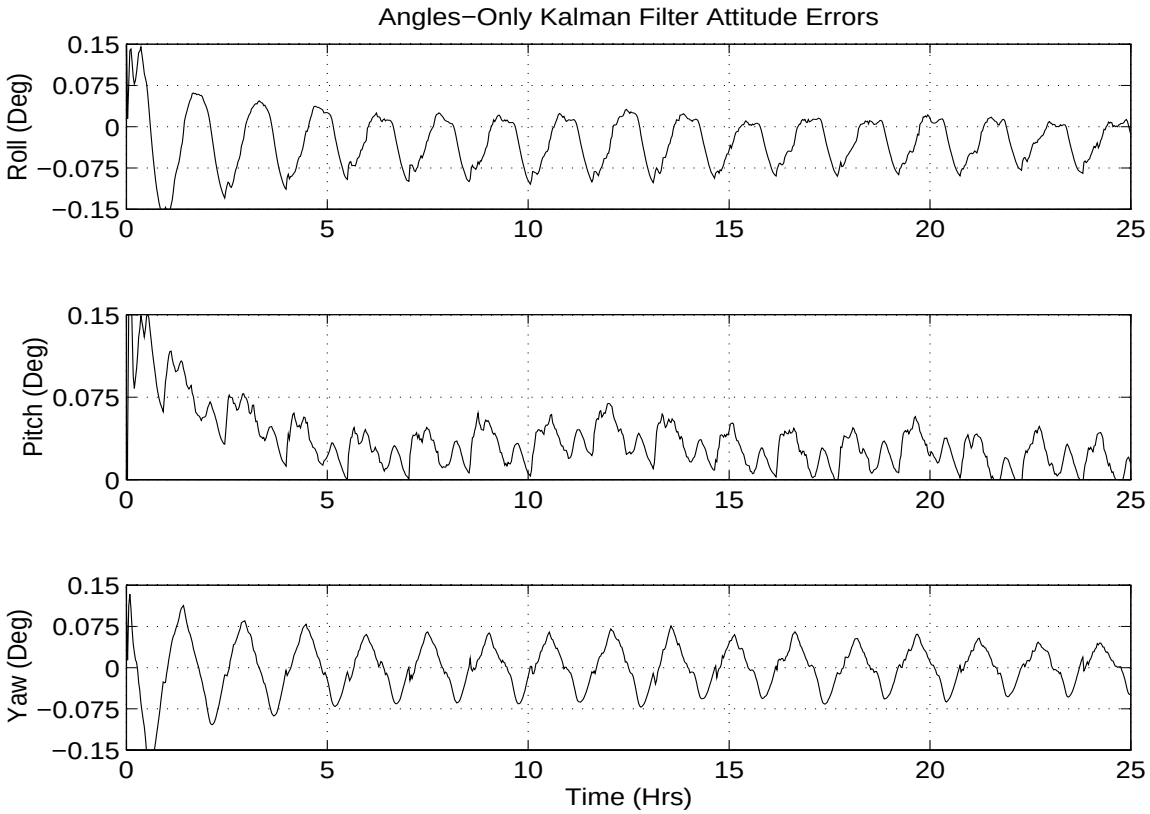

Figure 5 Angles-only Kalman Filter Attitude Errors

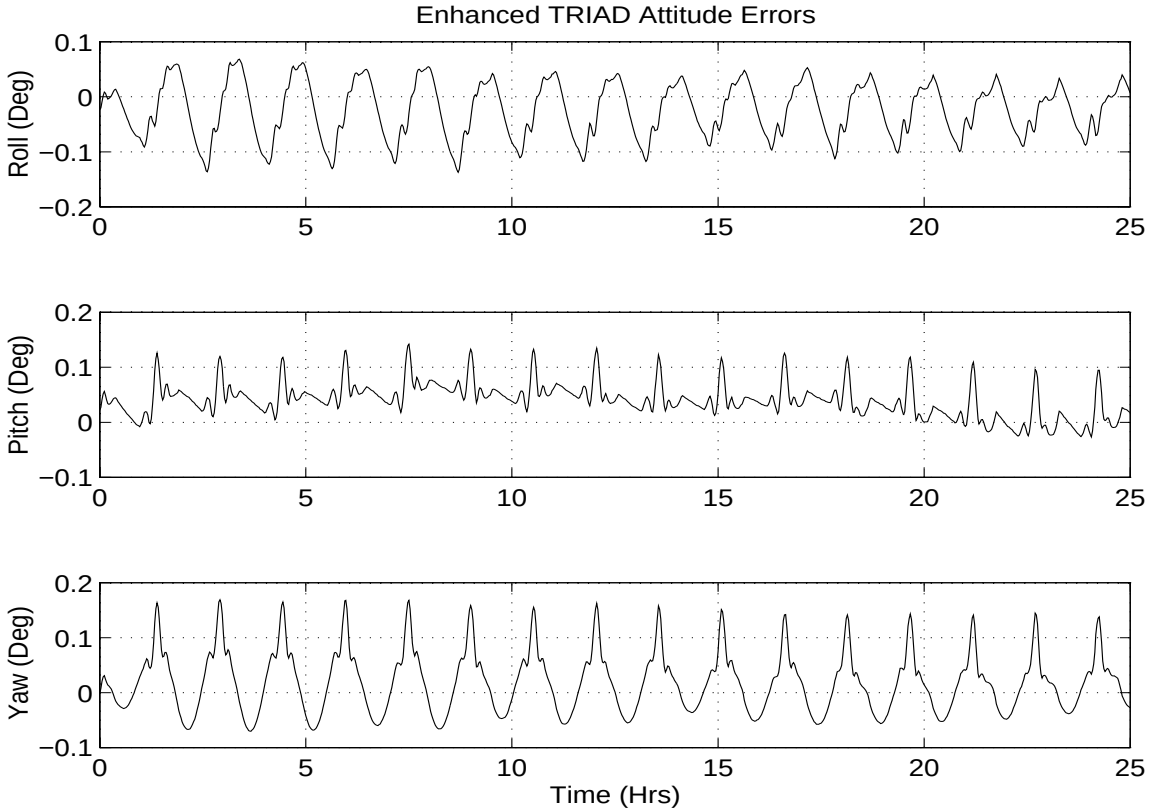

Figure 6 Enhanced TRIAD Attitude Errors

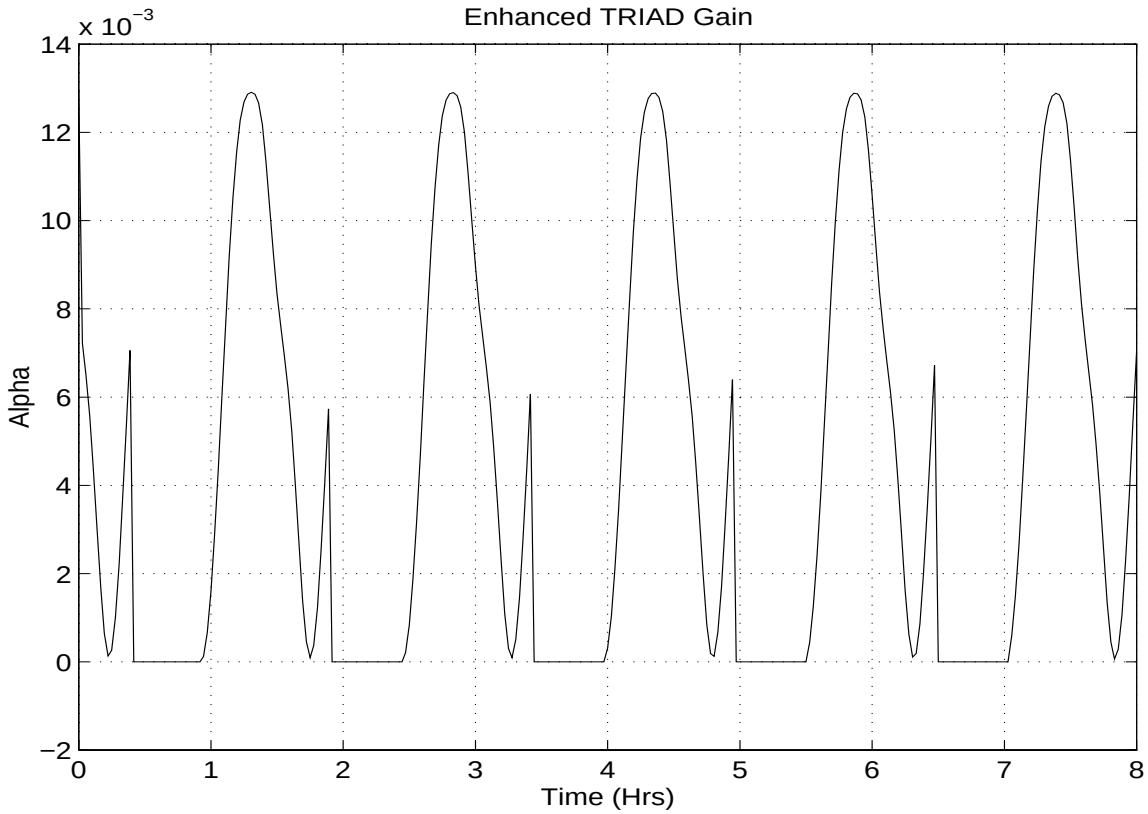

Figure 7 Enhanced TRIAD Filter Gain